GEOPHYSICAL RESEARCH LETTERS, VOL. 40, 4344–4348, doi:10.1002/grl.50844, 2013

Direct temperature and salinity acoustic full waveform inversion

G. Bornstein,[1] B. Biescas,[1,2] V. Sallarès,[1] and J. F. Mojica[1]

Received 28 June 2013; revised 1 August 2013; accepted 8 August 2013; published 22 August 2013.

[1] Recent work has shown that Full Waveform Inversion could be suitable to extract physical properties such as sound speed (c), density (ρ), temperature (T), and salinity (S) from the weak impedance contrasts associated with the ocean's thermohaline fine structure.The seismic inversion approaches proposed so far are based on the iterative inversion of c from multichannel seismic data, while the rest of parameters (T, S, and ρ) are determined in a second step using two equations of state and a local T-S empirical relationship. In this work, we present an alternative to this approach. Using 1-D synthetic seismic data, we demonstrate that the direct full waveform inversion of T and S using adjoint methods is feasible without the use of any local T-S relationship and that the models of physical properties obtained with this approach are far more accurate than those inferred from c. **Citation:** Bornstein, G., B. Biescas, V. Sallarès, and J. F. Mojica (2013), Direct temperature and salinity acoustic full waveform inversion, *Geophys. Res. Lett.*, *40*, 4344–4348, doi:10.1002/grl.50844.

1. Introduction

[2] Seismic oceanography is an acoustic method used to explore the thermohaline structure of the ocean's interior using multichannel seismic (MCS) systems [*Holbrook et al.*, 2003]. The amplitudes of the reflections at the horizons of the ocean's thermohaline fine structure depend on the acoustic impedance contrasts across these horizons, which are in turn a function of sound speed (c) and density (ρ) contrasts. Therefore, MCS data contains implicit information on the temperature (T) and salinity (S) structure. According to the Rayleigh principle, the potential vertical resolution of seismic data is $\sim \lambda/4$ (where λ is the wavelength that corresponds to the peak frequency of the seismic source), being between 1 and 10 m for conventional MCS systems. The theoretical lateral resolution, defined by the size of the first Fresnel zone, is between 10 and 100 m, depending on the frequency content of the seismic source used and the depth of the target, greatly improving the horizontal resolutions compared with more traditional oceanographic techniques.

[3] Until now, applications of inversion methodologies to oceanographic seismic data have centered on retrieving 1-D sound speed models from stacked MCS traces, using either local optimization methods such as full waveform inversion [*Wood et al.*, 2008; *Kormann et al.*, 2011] or processing-based approaches [*Papenberg et al.*, 2010], since it is the parameter with the strongest influence on the acoustic reflectivity [*Ruddick et al.*, 2009; *Sallarès et al.*, 2009]. In order to obtain the T and S models from a single c model, two additional equations are required: (i) an equation relating c with T, S, and depth (z), e.g., *Millero et al.* [1980]; and (ii) an empirical T-S relationship, which can be obtained from local or regional oceanographic data. Since a single T-S relationship should be used for all the seismic section, covering different mesoscale structures, this step can be a source of significant errors in this inversion approach.

[4] In this work, we propose and present a new full waveform inversion (FWI) approach, which resolves directly both T and S from a 1-D synthetic seismic trace without the need of a T-S relationship. FWI was originally proposed to extract information on the ground elastic properties from the complete seismic wavefield [*Lailly*, 1983; *Tarantola*, 1984] and is commonly formulated as a local optimization problem where the gradient of the inverted parameters is calculated based on adjoint techniques. We show that it is possible to implement sensitivity kernels allowing for the direct inversion of T and S, as they appear implicitly in the acoustic wave equation. In a second step, c and ρ can be retrieved through the equations of state, so the main oceanographic scalar physical parameters can be determined without additional approximations.

2. Method

[5] We have implemented a time domain, multiscale, 1-D acoustic FWI algorithm with a gradient-based optimization scheme that solves for c, ρ, T, and S. The sensitivity kernels of those parameters are calculated via the adjoint method, and we use the iterative nonlinear conjugate gradients (NL-CG) search method to minimize a misfit function.

[6] In order to explore the methodological limits of this method, we test the approach with synthetic data generated with a 1-D, time domain, finite-difference solver of the acoustic wave equation [*Kormann et al.*, 2010] applied on a model of the physical parameters to be recovered (target model). This means that the problems that are present in real seismic data inversion such as signal-to-noise ratio, source wavelet identification, and direct wave removal are avoided, and we can focus on the performance of the inversion and compare it with previously proposed schemes. The target models are obtained from real conductivity-temperature-depth (CTD) casts, and a low-pass filter is used to create the initial models.

[7] The nonhomogeneous acoustic wave equation is

$$\nabla\left[\frac{1}{\rho}\nabla u(z,t)\right]-\frac{1}{K}\frac{\partial^2 u(z,t)}{\partial t^2}=f_s(z,t) \quad (1)$$

where $f_s(z,t)$ is the acoustic source, which specifies the shape and time evolution of the source, K is the bulk modulus

[1]Institut de Ciencies del Mar, CSIC, Barcelona, Spain.
[2]Department of Oceanography, Dalhousie University, Halifax, Nova Scotia, Canada.

Corresponding author: G. Bornstein, Institut de Ciencies del Mar, CSIC, CMIMA, Passeig Maritim de la Barceloneta 37-49, 08003 Barcelona, Spain. (bornstein@icm.csic.es)

0094-8276/13/10.1002/grl.50844

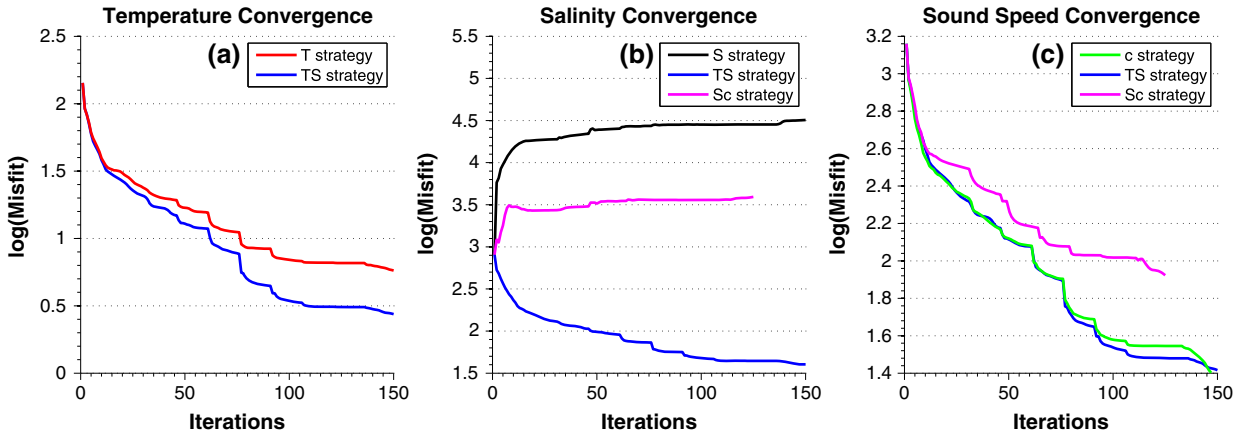

Figure 1. Semilogarithmic plot of the misfit convergence of each variable for the different strategies: *T* strategy (RMS = 0.1°C for *T*), *TS* strategy (RMS = 0.05°C for *T*, RMS = 0, 02 for *S*, and RMS = 0.2 m/s for *c*), *S* strategy (RMS = 0.4 for *S*), *Sc* strategy (RMS = 0.1 for *S* and RMS = 0.4 m/s for *c*), and *c* strategy (RMS = 0.3 m/s for *c*).

($K = \rho c^2$), and $u(z,t)$ is the pressure signal or seismic trace. To simulate the data with the acoustic solver, we locate the source and receiver both at 20 m depth. The source wavelet chosen is a Ricker wavelet with peak frequency of 75 Hz, which mimics the signal that is produced in the MCS experiments. It must be noted that having an accurate estimation of the source wavelet is key for a successful FWI. There are different approaches to determine and refine the wavelet based on processing, modeling, or even FWI [*Pratt*, 1999; *Shin et al.*, 2007], but this issue is beyond the scope of this work and we assume that the source wavelet is known.

[8] The misfit (M) is the difference between the reference seismic trace (u_0) and the one computed with the initial (or updated) model at the receiver location ($u(m)$). We use the Euclidean norm or least squares criterion as misfit

$$M(u_0,u;m) = \frac{1}{2}\sum_{i}^{N}\left[u^i(m) - u_0^i\right]^2 \tag{2}$$

where u_0 and $u(m)$ are the real and modeled seismic data, respectively, m is the parameter model, and N is the number of discrete temporal sample points of the seismic traces.

[9] The adjoint method is a mathematical tool used to compute the gradient (or Fréchet sensitivity kernel) of the misfit function with respect to any physical parameter in the direction δm [*Tarantola*, 1984; *Fichtner et al.*, 2006; *Fichtner*, 2011]:

$$\nabla_m M \delta m = \int \text{kernel}_m \delta m \, \mathrm{d}^3x \tag{3}$$

where the spatial integral is over the location of the receivers. Commonly, the kernels are derived for the parameters that appear explicitly in the acoustic equation (K and ρ) [*Tarantola*, 1984; *Fichtner et al.*, 2006; *Kormann et al.*, 2011], but it is also possible to compute the kernels for other parameters functionally related to K and ρ, such as c, T, and S. Following *Fichtner et al.* [2006], the kernels that we will use for the analysis are

$$\text{kernel}_\rho = \left\langle \frac{1}{\rho^2}, \nabla u \nabla \psi \right\rangle \tag{4}$$

$$\text{kernel}_c = -\left\langle \frac{1}{\rho c}, \nabla u \nabla \psi \right\rangle - \left\langle \frac{1}{Kc}, \partial_t u \partial_t \psi \right\rangle \tag{5}$$

$$\text{kernel}_T = \left\langle \frac{1}{\rho^2}\partial_T \rho, \nabla u \nabla \psi \right\rangle - \left\langle \frac{1}{K^2}\partial_T K, \partial_t u \partial_t \psi \right\rangle \tag{6}$$

$$\text{kernel}_S = \left\langle \frac{1}{\rho^2}\partial_S \rho, \nabla u \nabla \psi \right\rangle - \left\langle \frac{1}{K^2}\partial_S K, \partial_t u \partial_t \psi \right\rangle \tag{7}$$

where the brackets mean a temporal integral over the measurement time interval. ψ corresponds to the adjoint wavefield, which is calculated by a back propagation of the misfit from the receiver to the source locations.

[10] Finally, the optimization problem searches for the best direction and step size in order to minimize the misfit. We have implemented a nonlinear Conjugated Gradient method (NL-CG) that uses the gradient previously obtained to provide the search direction. Using a parabolic approximation around the misfit minimum, an optimal step size can be calculated, complementing the search direction to find the minimum misfit.

[11] Due to the strong nonlinearity of the FWI problem, and in order to find the global misfit minimum and not a local one, a hierarchical multiscale strategy [*Bunks et al.*, 1995] has been implemented. By low-pass filtering, the seismic data on each iteration at the desired frequency, following a predefined frequency strategy, the nonlinearity can be mitigated. The lowest model wave numbers (the lowest frequency in the data) are resolved, and sequentially, the model details are increased using the solution obtained at a given frequency as initial model for the next one.

3. Results

3.1. Full Waveform Inversion Strategies

[12] The reference T, S, c, and ρ models used in the inversion were acquired with a CTD during the Geophysical Oceanography (GO) survey that took place in April-May of 2007 in the Gulf of Cádiz [*Hobbs*, 2009]. The initial models were generated by low-pass filtering the reference model with a cutoff frequency of 3.75 Hz, the lowest frequency that gave optimal results after several tests. The synthetic seismic signal, u_0, was obtained by the acoustic propagation through the CTD profile and input to the FWI process. The inversion followed this multiscale frequency strategy:

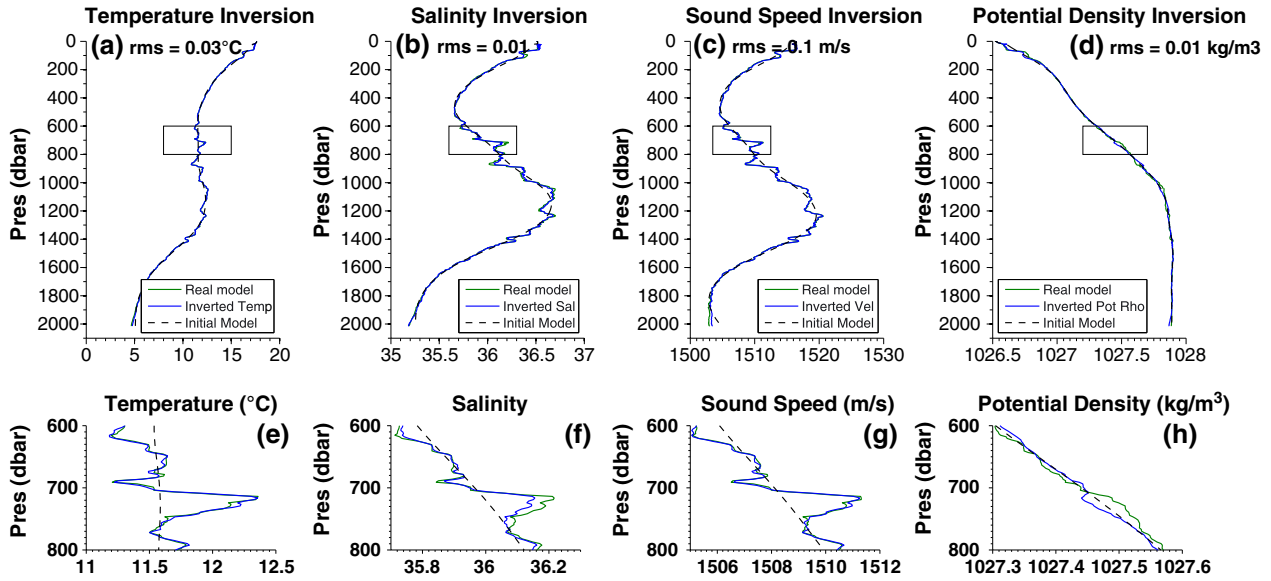

Figure 2. Initial, real, and inverted models of (a) temperature, (b) salinity, (c) sound speed, and (d) potential density and the corresponding RMS values of the difference between real and inverted profiles. (e–h) Detail of the thermohaline structure for each parameter.

[4, 4.5, 5, 6, 8, 16, 32, 64, 75, 4] Hz, with a maximum of 15 iterations of the NL-CG scheme at each frequency step.

[13] The following combination of variables were tested for the inversion: T, TS, Tc, S, Sc, c, ρ, $c\rho$, and $T\rho$ in order to determine the best inversion performance. The comparison between inversions was analyzed in terms of the rate of convergence of the misfit of the parameters inverted in each strategy. Inverting ρ proved impossible, as the difference between the updated and the real model (model misfit) increases at each iteration for all the cases studied, proving that the variability of the density in the ocean cannot be retrieved by means of the FWI. *Ruddick et al.* [2009] and *Sallarès et al.* [2009] already showed in their works that the contribution of the density changes to the reflectivity in the ocean is negligible in comparison with the rest of the variables. Therefore, we decided to discard this variable and study the strategies based on the other three: c, T, and S and their combinations in pairs. The simultaneous inversion of two variables is optimized if they have complementary contributions to the reflectivity. When represented on a T-S diagram, c is almost parallel to T, a fact that is not compatible with our search of complementarity and lead us to discard this combination of variables and focus on the more suitable combinations TS and Sc.

[14] Figure 1 shows the main results of the inversion tests and the root-mean-square (RMS) residual between the final inversion model and the CTD data. In all cases considered, the TS strategy provides the best results. This strategy is key to properly retrieve S (Figure 1b), because the S and Sc strategies fail to minimize the model misfit. The c strategy used in previous works performs similarly well to retrieve c (Figure 1c). This could be an alternative to the TS inversion, but it has an important weakness, which is the need of an extra T-S relationship to estimate T and S.

[15] In terms of convergence, the TS strategy clearly provides the best results for the FWI method applied to the ocean. This could be explained by the results presented in *Sallarès et al.* [2009], in which T and S are the parameters with a more equilibrated contribution to the ocean's reflectivity (80% and 20% on average, respectively), leading to a more symmetric misfit function which improves the performance of the NL-CG optimization. Figure 2 shows the comparison of the final TS inversion and the original CTD profiles for the four analyzed physical properties. Sound speed and potential density (ρ_θ) were derived apply-

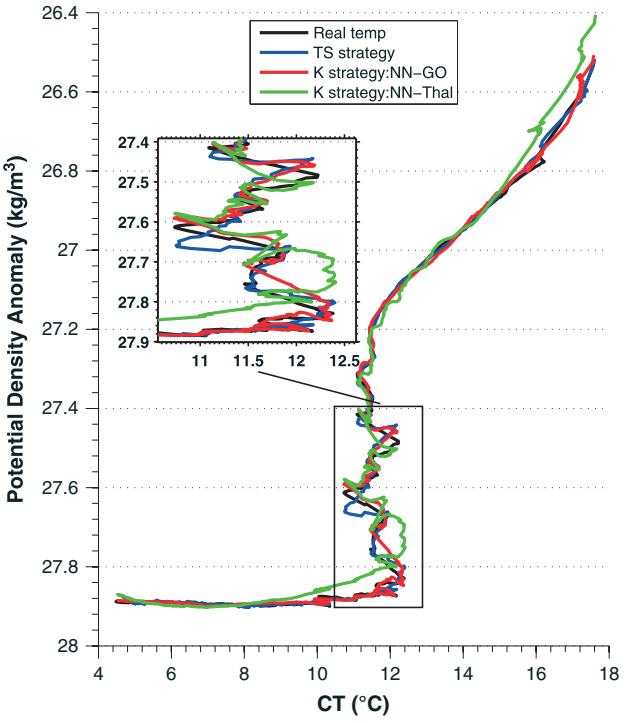

Figure 3. Real model and inverted models for TS strategy and K strategy with two different neural networks (GO and Thalassa) in a conservative temperature versus potential density plot.

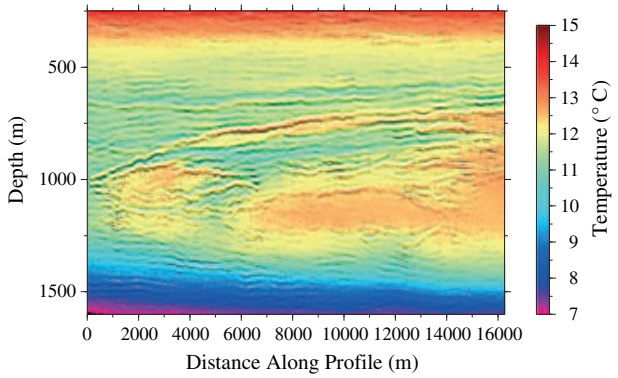

Figure 4. Temperature profile illuminated by the seismic data, obtained by propagating the acoustic solver over the temperature and salinity profiles calculated in *Kormann et al.* [2011].

ing the equations of state to the inverted T and S. The method resolves the vertical profiles with a RMS of 0.03°C, 0.01, 0.1 m/s, and 0.01 kg/m^3 for T, S, c, and ρ_θ, respectively, which are twofold to threefold smaller than the RMS obtained following the K strategy proposed by *Kormann et al.* [2011] (combination of K inversion, equations of state and local T-S) using the same data: 0.1°C for T, 0.02 for S, and 0.3 m/s for c.

3.2. Estimation of Potential Density

[16] Potential density is an important dynamic property of the ocean, as it addresses the stability of the water column. Therefore, ρ_θ can establish an important difference between inversion results, helping to determine which of them complies better with the dynamic behavior found in the ocean. It is strongly affected by the empirical T-S relationship, or in its absence, by the relation between the inverted T and S, since a wrongly compensation could sum up the errors and lead to higher error in potential density [*Stommel*, 1979; *Rudnick and Ferrari*, 1999]. Therefore, we tested our strategies in thermohaline intrusions, structures where conservative temperature (CT) varies along constant ρ_θ lines (Figure 3). We overlapped the CTD data with the results of the *TS* strategy and the K strategy [*Kormann et al.*, 2011], the later using two different T-S relationships: *NN-GO*, trained with CTDs that were coincident to the seismic data acquisition during the GO cruise [*Hobbs*, 2009], and *NN-Thal*, trained with noncoincident CTDs, which belong to the Thalassa Leg2 Cruise, that took place in the same area, but 10 years before. In terms of potential density, this plot clearly displays the similar performance of the *TS* strategy and the K strategy with the very well suited *T-S*:*NN-GO* and reveals the errors derived from the quality of the T-S relationship. The *T-S*:*NN-Thal* shows lower accuracy in all the potential density profile, supporting the evidence that the inversion results are particularly sensitive to the lack of an optimal T-S relationship, and thus confirming the suitability of the *TS* strategy.

3.3. Coincidence of Reflectors and Isotherms Along the GO-LR 10 Line

[17] As a way to present some of the possibilities of the retrieval of oceanographic parameters from MCS, we applied the FWI scheme presented here to the GO-LR 10 line acquired during the GO survey [*Hobbs*, 2009]. Using as target models, the result obtained by *Kormann et al.* [2011], we propagated the solver of the acoustic wave to each trace in order to obtain a seismic profile of the line. Next, by means of parallel computing, we inverted each trace for T and S, obtaining two profiles more than 16 km long of both parameters with a horizontal resolution of 6.25 m.

[18] In Figure 4, we present the temperature profile illuminated by the seismic data. The T gradients follow precisely the seismic reflectors, supporting the evidence that the ocean's reflectivity is mainly determined by the T contrasts [*Ruddick et al.*, 2009].

4. Conclusions

[19] We have presented a new strategy for the direct FWI of T and S from seismic oceanography data. The Fréchet sensitivity kernels of both parameters are incorporated into a FWI scheme with a local optimization strategy. The main innovation of our work with respect to all the previous inversions is that our method directly inverts T and S from the wave equation. An important advantage of this approach is that local empirical relationships are not required to determine the model of physical parameters. Results prove the ability of this new approach to invert T, S, and the rest of related oceanographic parameters such as c or ρ_θ, with twofold to threefold better accuracy than those obtained from the conventional inversion of c or K using the same data. Next steps will be to implement the FWI algorithm in 2-D in order to invert data in the shot gather domain rather than in the stacked domain, include the source inversion and applying it to real data.

[20] **Acknowledgments.** The principal author wishes to thank Jean Kormann, Naiara Korta, and Daniel Dagnino for their generous contributions that helped carrying out this work. The comments of Andreas Fichtner and an anonymous reviewer helped to improve the manuscript. We acknowledge the EU-funded GO-project (EC-NEST-15603) as well as the German funded POSEIDON CRUISE (P350) for providing the experimental data set. This work has been fulfilled in the framework of the project POSEIDON (CTM2010-25169) and APOGEO (CTM2011-16001-E/MAR), both funded by the Spanish Ministry of Economy and Competitiveness (MINECO), and the Marie Curie project OCEANSEIS (FP7-PEOPLE-2010-IOF-271936-OCEANSEIS).

[21] The Editor thanks Andreas Fichtner and an anonymous reviewer for their assistance evaluating this paper.

References

Bunks, C., F. M. Saleck, S. Zaleski, and G. Chavent (1995), Multiscale seismic waveform inversion, *Geophysics*, *60*(5), 1457–1473.

Fichtner, A. (2011), *Full Seismic Waveform Modelling and Inversion*, Springer, Berlin Heidelberg.

Fichtner, A., H.-P. Bunge, and H. Igel (2006), The adjoint method in seismology. I. Theory, *Phys. Earth Planet. Inter.*, *157*, 86–104, doi:10.1016/j.pepi.2006.03.016.

Hobbs, R. (2009), GO-Geophysical Oceanography: A new tool to understand the thermal structure and dynamics of the ocean, *EC-NEST 15603*, Durham Univ., Durham, U. K.

Holbrook, W. S., P. Páramo, S. Pearse, and R. W. Schmitt (2003), Thermohaline fine structure in an oceanographic front from seismic reflection profiling, *Science*, *301*(5634), 821–824, doi:10.1126/science.1085116.

Kormann, J., P. Cobo, B. Biescas, V. Sallarès, C. Papenberg, M. Recuero, and R. Carbonell (2010), Synthetic modelling of acoustical propagation applied to seismic oceanography experiments, *Geophys. Res. Lett.*, *37*, L00D90, doi:10.1029/2009GL041763.

Kormann, J., B. Biescas, N. Korta, J. de la Puente, and V. Sallarès (2011), Application of acoustic full waveform inversion to retrieve high-resolution temperature and salinity profiles from synthetic seismic data, *J. Geophys. Res.*, *116*, C11039, doi:10.1029/2011JC007216.

Lailly, P. (1983), The seismic inverse problem as a sequence of before stack migrations, in *Conference on Inverse Scattering: Theory and*

Application, edited by J. B. Bednar et al., 206–220, Soc. Industr. Appl. Math., Philadelphia, Pa.

Millero, F. J., C.-T. Chen, A. Bradshaw, and K. Schleicher (1980), A new high pressure equation of state for seawater, *Deep Sea Res., Part A*, *27*(3-4), 255–264.

Papenberg, C., D. Klaeschen, G. Krahman, and R. W. Hobbs (2010), Ocean temperature and salinity inverted from combined hydrographic and seismic data, *Geophys. Res. Lett.*, *37*, L04601, doi:10.1029/2009GL042115.

Pratt, G. (1999), Seismic waveform inversion in the frequency domain, Part 1: Theory and verification in a physical scale model, *Geophysics*, *64*(3), 888–901.

Ruddick, B., H. Song, C. Dong, and L. Pinheiro (2009), Water column seismic images as maps of temperature gradient, *Oceanography*, *22*(1), 192–205.

Rudnick, D. L., and R. Ferrari (1999), Compensation of horizontal temperature and salinity gradients in the ocean mixed layer, *Science*, *283*(5401), 526–529, doi:10.1126/science.283.5401.526.

Sallarès, V., B. Biescas, G. Buffett, R. Carbonell, J. J. Dañobeitia, and J. L. Pelegrí (2009), Relative contribution of temperature and salinity to ocean acoustic reflectivity, *Geophys. Res. Lett.*, *36*, L00D06, doi:10.1029/2009GL040187.

Shin, C., S. Pyun, and J. B. Bednar (2007), Comparison of waveform inversion, Part 1: Conventional wavefield vs logarithmic wavefield, *Geophys. Prospect.*, *55*, 449–464.

Stommel, H. (1979), Determination of water mass properties of water pumped down from the Ekman layer to the geostrophic flow below, *Proc. Natl. Acad. Sci. U.S.A.*, *76*(7), 3051–3055.

Tarantola, A. (1984), Linearized inversion of seismic reflection data, *Geophys. Prospect.*, *32*, 998–1015.

Wood, W. T., W. S. Holbrook, M. K. Sen, and P. L. Stoffa (2008), Full waveform inversion of reflection seismic data for ocean temperature profiles, *Geophys. Res. Lett.*, *35*, L04608, doi:10.1029/2007GL032359.